Available online at www.sciencedirect.com
SCIENCE DIRECT®
Catalysis Today 89 (2004) 279–286
CATALYSIS TODAY
www.elsevier.com/locate/cattod

Characterization of lalithe, a new bentonite-type Algerian clay, for intercalation and catalysts preparation

L.S. Belaroui [a,*], J.M.M. Millet [b], A. Bengueddach [a]

[a] *LCMO, Université d'Oran, BP 1524 Oran, El M'Naouer, Algeria*
[b] *Institut de Recherche sur la Catalyse, CNRS, 2 av. A. Einstein, 69626 Villeurbanne, France*

Abstract

Iron-intercalated clay has been obtained starting from a natural bentonite-type clay sample from Maghnia (Algeria). The natural compound contained, besides the clay material, impurities such as quartz, β-cristobalite and calcite. The quartz phase was removed by applying a purification protocol based on sedimentation. The two other phases remained in the solid but did not apparently affect the intercalation process.

The intercalation process has been optimized to lead a microporous solid with a reticular distance of 16 Å and a specific surface area of 260 $m^2 g^{-1}$. High-resolution electron microscopy with EDX analyses showed that the sample had a relatively inhomogeneous composition with a typical delaminated structure. It confirmed the pillaring but also showed some goethite particles. These particles certainly formed because of the delamination are few and small and do not affect the Mössbauer spectra showing only one ferric iron species and confirming that most of the iron was in the pillars.

The thermal stability of the iron-pillared clay has been studied. It was shown that the structure started to collapse before 773 K which is rather low for polyoxocations-intercalated clay but comparable for other iron-intercalated clays.

Keywords: Natural bentonite; Intercalation; Delaminated clays; Iron-pillared clays

1. Introduction

Clays, which have always been commonly used as catalysts, are attracting the attention of researchers as they represent a class of materials which porosity may be tailored by intercalation. Their pore openings generally vary from 4 to 22 Å depending upon the size and type of the pillars used which allows the adsorption and further conversion of large organic molecules. The pillared clays are prepared by insertion in the interlamellar space of montmorillonite of various metal polycations, which after calcination transform into rigid pillar oxides giving a homogeneous distribution of micropores.

The most important studies on pillared clays began in 1973 with the use for the intercalation of Al hydroxycations corresponding to Al_{13} polymeric species and leading to interlamellar space of 18 Å [1]. Since then numerous works have been realized on the exchanged montmorillonite with polycations of various metals such as Al [2–4], Fe [5–12], Ti [13,14], Zr [15–17] or V [18]. These polycations which are polarized by coordinated water molecules give by hydrolysis protons in the interlamellar space as in the case of iron:

$$[Fe(OH_2)_{2n}]^{n+} \rightarrow [Fe(OH_2)_{2n-1}(OH)]^{(n-1)+} + H^+ \quad (1)$$

It was shown that the clay catalysts contained at the same time Lewis acid and Brønsted sites [19,20]. The Brønsted acidity is very much influenced by the water quantity between the layers of the exchanged clay. Indeed, after calcination at 573 K, most clays start to collapse and one notes a decrease in the Brønsted acidity with an increase in the Lewis acidity.

In this work, we are presenting the synthesis and physicochemical characterization of a delaminated iron-clay prepared from a natural Algerian bentonite. The study has focused on the structure and textural characteristics needed for a catalytic application and their thermal stability.

* Corresponding author. Fax: +213-41-32-2880.
E-mail address: lbelaroui@algeriecom.com (L.S. Belaroui).

0920-5861/$ – see front matter © 2004 Elsevier B.V. All rights reserved.
doi:10.1016/j.cattod.2003.12.020

2. Experimental

2.1. Materials

The starting clay used was a bentonite from Maghnia, which is a natural clay mineral with a (0 0 1) spacing of 10 Å. It owns to the montmorillonite family which are aluminosilicates of 2/1 type with a theoretical formula $M_xSi_4O_{10}(Al_{2-x}R_x)(OH)_2{\cdot}nH_2O$, with M and R corresponding, respectively, to monovalent and divalent cations. The number of water molecules (n) and the extent of substitution (x) can vary from a compound to the other and the cation M can also correspond in some cases to divalent or trivalent cations.

Before being used for intercalation, the bentonite was purified. Ten grams of the natural clay were ground, sieved to 40 μm and dried at 378 K. They were then dispersed into 1 l of distilled water for 2 h and allowed to settle for 16 h. The first 450 ml of the suspension was separated from the bottom and dried at 313 K. The calculated yields were very low and never exceed 10%. The bentonite material thus prepared was called lalithe.

2.2. Intercalation procedure

A 1 wt.% suspension of the colloid clay was first prepared by dispersing the purified bentonite into water under stirring. Parallel water solution of ferric nitrate ($Fe(NO_3)_3{\cdot}9H_2O$, 99.99%; Aldrich) was prepared and titrated with a base solution (Na_2CO_3). The solution was characterized by a Fe/OH molar ratio equal to 2. The titration was proceeded under vigorous stirring and was followed by an aging period of several hours at room temperature.

The iron containing solution was slowly added at room temperature to the clay suspension. The relative volume of the two solutions was chosen to have a final iron to clay ratio equal to 5 mmol g^{-1}. After the intercalation was completed, the flocculating clay was left in situ to age for about 18 h before washing by distillated water. The intercalated clay was then filtered using a plate and frame press.

To study the thermal stability of the clays, samples have been calcined under air at temperatures varying from room temperature to 773 K. The solids were heated at a rate of approximately 1 K min^{-1} and maintained at the chosen temperature for 5 h.

2.3. Characterization techniques

The structure of the clays before and after intercalation was studied by X-ray diffraction using a Phillips PW 3710 diffractometer using Cu Kα radiation. XRD patterns were recorded with 0.02° (2θ) steps over the 2–5° angular range with 1 s counting time per step. These recordings allowed to calculate the $d_{(0\,0\,1)}$-spacing characteristic of the interlamellar spacing for a pillared clay. Nitrogen adsorption/desorption measurements, carried out in a ASAP 2000 Sorptomatic, allowed to characterize the porosity of the products. The specific surface area was estimated using the BET method with adsorption data obtained in the reduced pressure range ($0.01 < P/P_0 < 0.15$) to avoid mistakes due to the condensation of N_2 in very small pores at relative pressures. The specific pore volume was also estimated at reduced pressure and the micropore volume calculated using the t-plot method. The porous distribution of the solids was determined using the BJH method, which allowed to calculate average pore diameters.

Differential thermal analyses (DTA) and thermogravimetric analyses (TG) were performed simultaneously using a SETARAM TGA-DTA 92 thermobalance coupled to a Balzers 420 QMC mass spectrometer. Thirty to sixty milligrams of the samples was placed in a platinum crucible suspended from one arm of the balance. The analyses were conducted at atmospheric pressure under an air flow (1 l h^{-1}) with a heating rate of 5 K min^{-1} and a temperature limit of 800 K. The precision of the thermogravimetric analyses was about 2%.

High-resolution electron microscopy was performed with a JEM 2010 (C_s = 0.5 mm). Accelerating voltage was 200 kV with a LaB_6 emission current, a point resolution of 0.195 nm and a useful limit of information of 0.14 nm. The instrument was equipped with an EDS LINK-ISIS (spatial resolution: 1 nm). A study by EDX has been conducted using a probe size of 25 nm to analyze isolated grains of the materials. Standard deviations were evaluated for atomic ratios from at least 20 analyses. The Mössbauer spectra were recorded at room temperature, using a 2 GBq $^{57}Co/Rh$ source and a conventional constant acceleration spectrometer, operated in triangular mode. The isomer shifts (δ) were given with respect to α-Fe and were calculated as the quadrupole splitting (Δ) and the line width (W), with a precision of about 0.02 mm s^{-1}.

3. Results and discussion

3.1. Characterization of the starting materials

The chemical composition of the natural bentonite has been determined, which is presented in Table 1. The relative

Table 1
Chemical analysis of the natural bentonite sample as extracted

	Composition (wt.%)
SiO_2	65.20
Al_2O_3	17.25
MgO	3.10
Na_2O	2.15
Fe_2O_3	2.10
CaO	1.20
K_2O	0.60
TiO_2	0.20
H_2O	8.20

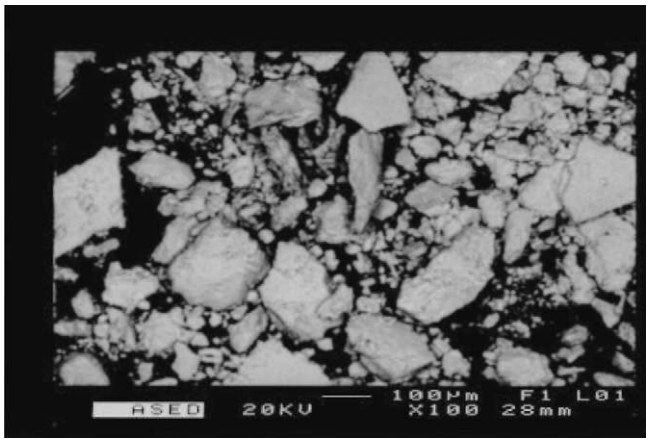

Fig. 1. Microphotograph of the clay after the purification process showing the agglomeration of the particles.

content of divalent cations (Ca, Mg) was rather high and since substitution levels in the octahedral sheet are generally limited to a maximum of one-forth of the cations, the later cations should occupy monovalent cation sites with certainly some trivalent cations. It can be noticed that the iron content of solid was rather low compared to other similar materials. After the purification process, the solid obtained have been characterized by SEM and X-ray diffraction. SEM pictures showed only particles that are strongly agglomerated whose diameter was $\leq$1.6 μm (Fig. 1). The purification process thus has a sifting effect on the solids. The material thus prepared was characterized by a $d_{(001)}$-spacing equal to 12.6 Å. Impurities such as quartz have been eliminated but the solids always contained small amounts of calcite and β-cristobalite (Table 2). The bentonite has been characterized by DTA–TG analysis before and after purification and after iron pillaring. The mass loss and heat flow curves obtained are shown in Fig. 2. We can see on the natural compound, between room temperature and 350 K, the departure of adsorbed hydration water and, between 350 and 430 K, the departure of the water located between the layers of the clay. A water loss was also observed around 460 K that may be attributed to iron or aluminum hydroxides that will be removed during the purification process. The dehydroxylation of the natural compound seemed to take place after 600 K.

Table 2
XRD characterization data of the starting clays

Starting bentonite		Purified and sifted bentonite (lalithe)	
d (Å)	hkl	d (Å)	hkl
14.71	001	12.6	001
5.15	101; β-cristobalite	4.95	101; β-cristobalite
4.50	020, 110	4.43	020, 110
3.76	004		
3.35	011; quartz (low form)		
3.02	104; calcite	3.03	104; calcite
2.55	200, 130	2.53	020, 110

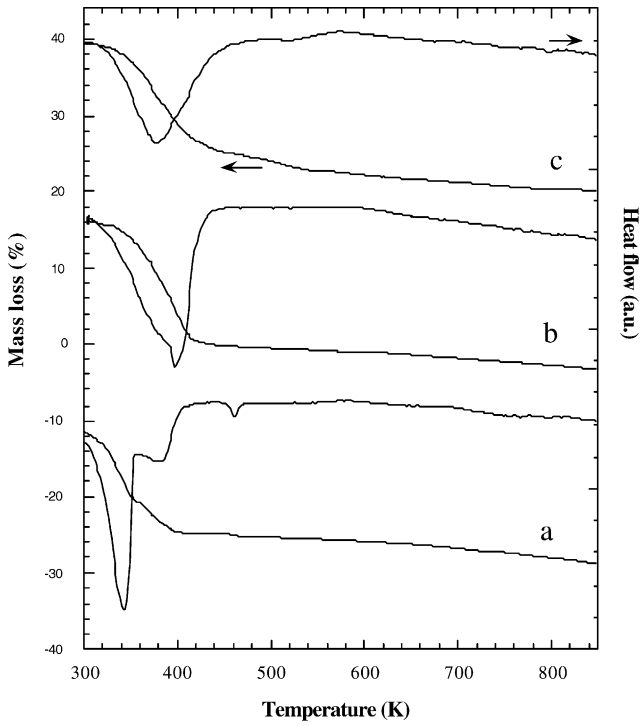

Fig. 2. TG and DTA curves for the clay (a) before and (b) after the purification process and (c) after intercalation.

The purified compound did not appear hydrated but contained more interlayer water, which was lost up to 440 K. The dehydroxylation started as for the natural compound around 600 K. After iron pillaring, the solid contained always water between the layer, which was lost between room temperature and 460 K. The smaller water departure around 530 K which was not observed in the other compounds may be attributed to a partial dehydration of the pillars. It should be mentioned that the TG analyses showed a water weight loss of about 14%, which was slightly higher than the result of chemical analysis. However, it is known that the hydration of clay could vary depending upon the conditions of stocking and the sampling.

3.2. Textural and structural properties of the intercalated clay

The results of the textural characterization of the lalithe sample before and after intercalation are gathered in Table 3

Table 3
Physicochemical characteristic of the clay determined before and after intercalation

Specific characteristics	Starting lalithe	Lalithe after intercalation
$d_{(001)}$-Spacing (Å)	12.6	16
BET surface area ($m^2\,g^{-1}$)	10.5	260
Surface area of micropores ($m^2\,g^{-1}$)	–	85.7
Micropore volume ($cm^3\,g^{-1}$)	–	40
Average pore diameter (Å)	96	25
Fe content (wt.%)	2.4	34.8

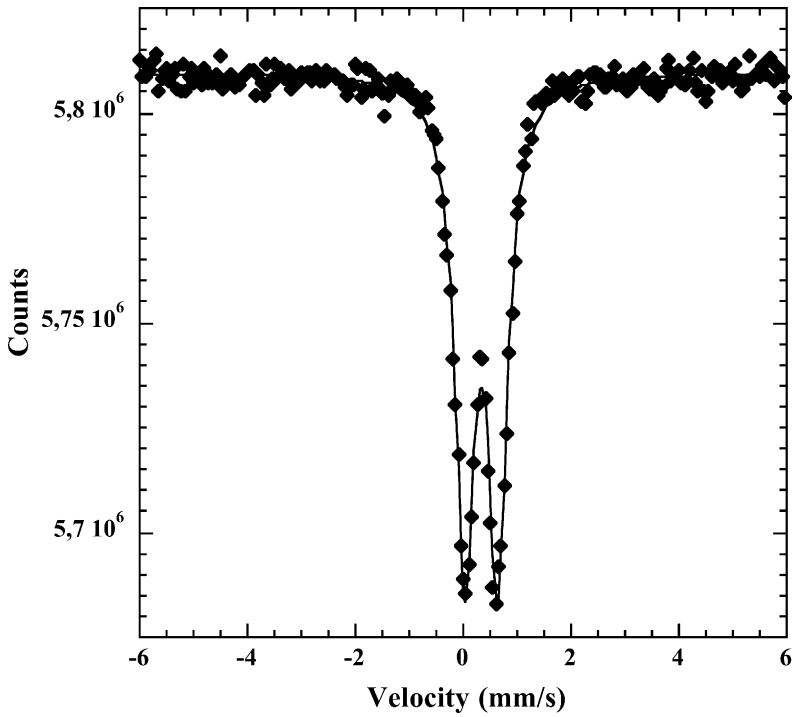

Fig. 3. Experimental Mössbauer spectrum of the iron-pillared clay recorded at 295 K. Solid lines are derived from least-square fits.

with their $d_{(0\,0\,1)}$-spacing calculated from XRD data. These data correspond to the best results obtained with intercalation duration of 2 h and an iron/clay ratio of 5 mmol g^{-1}. We can see that the intercalation well occurred with a $d_{(0\,0\,1)}$-spacing increasing from 12.6 to 16 Å. At the same time, the specific surface area increased from about 10 to 260 $m^2\,g^{-1}$.

The structure of the Fe pillars is unknown but the size of the pillars of about 16–18 Å is compatible with a

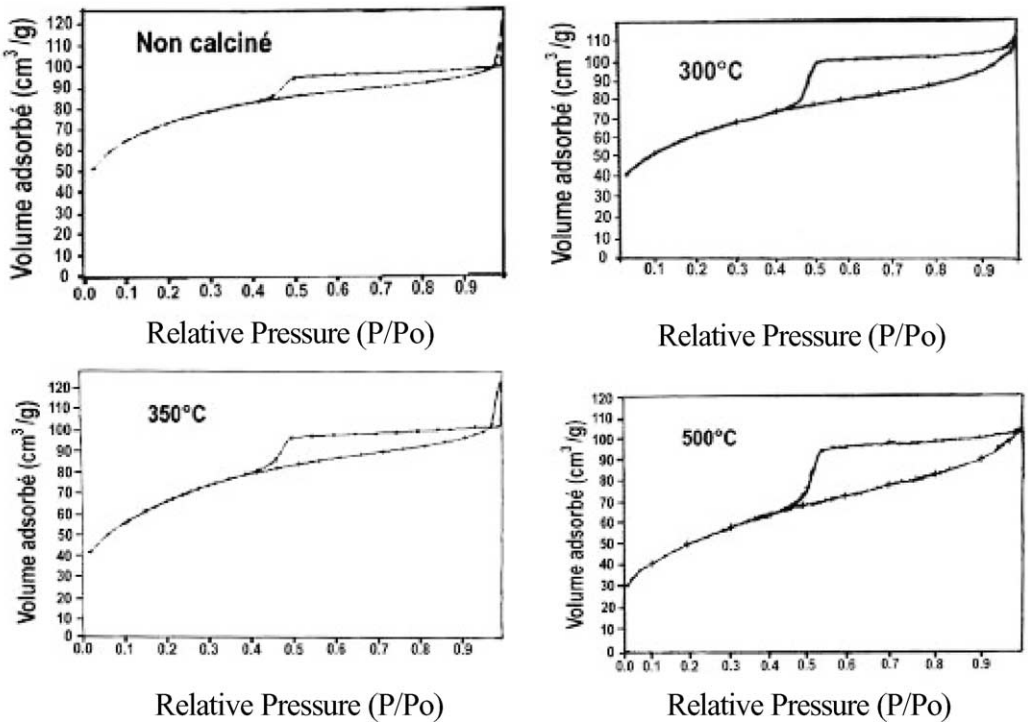

Fig. 4. Isotherms of adsorption–desorption of iron-pillared lalithe material heat-treated at various temperatures.

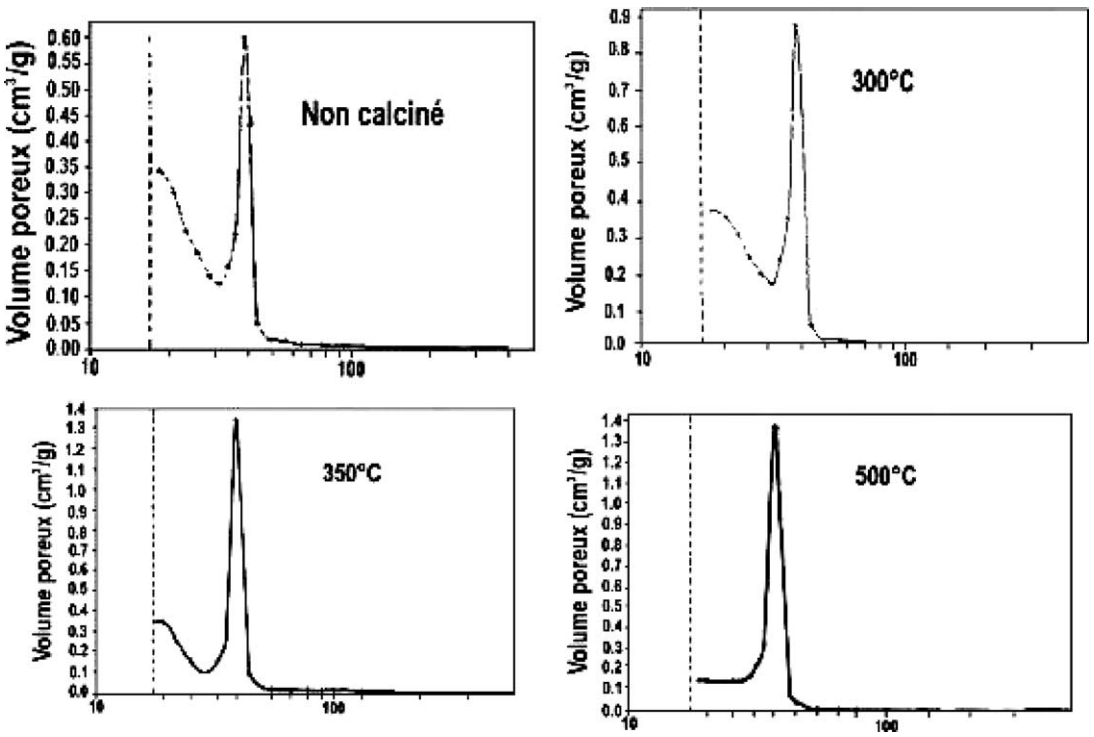

Fig. 5. Distribution of the porous distribution of iron-pillared lalithe material heat-treated at various temperatures.

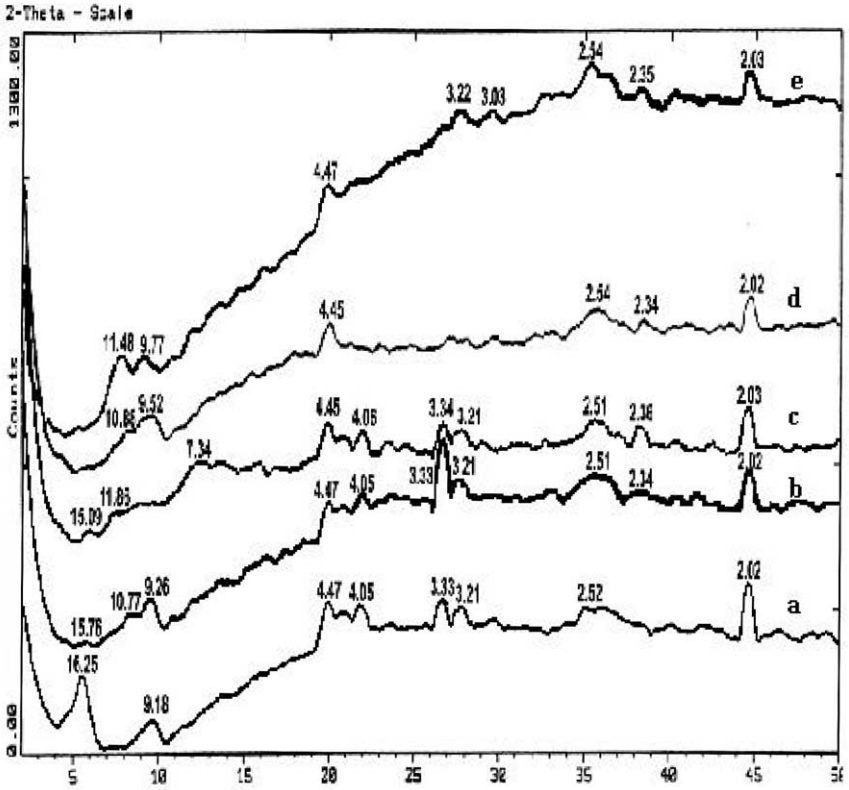

Fig. 6. X-ray powder diffraction patterns of iron-pillared lalithe material heat-treated at various temperatures: (a) room temperature, (b) 473 K, (c) 573 K, (d) 623 K and (e) 773 K.

Table 4
Calculated Mössbauer parameters from the spectrum of the iron-intercalated clay

Site	Fe^{3+}
δ (mm s^{-1})	0.36
W (mm s^{-1})	0.42
Δ (mm s^{-1})	0.61

δ: isomeric shift (referred to αFe); W: line width; Δ: quadrupolar splitting.

trinuclear, octahedral corner-sharing complex $Fe_3(OH)_a(H_2O)_b$ with $a + b = 16$ and a/b ratio depending upon the exchange mechanism. The structure of these clusters should be related to that of ferrihydrite $Fe_5O_7OH{\cdot}4H_2O$ whose conditions of formation corresponded to that of the intercalation. It could be recalled that this last phase was clearly identified in other iron-containing-type of lamellar compounds like hydrocalcite [21]. The specific surface areas measured were in good agreement with those determined for other iron-pillared clays reported in the literature [7,22]. The Mössbauer spectrum of the iron-pillared material, presented in Fig. 3, shows only two peaks corresponding to a ferric doublet. The parameters calculated from the fit of this doublet were consistent with high-spin Fe^{3+} in octahedral environment (Table 4). They corresponded well to those published for the same type of compound [23].

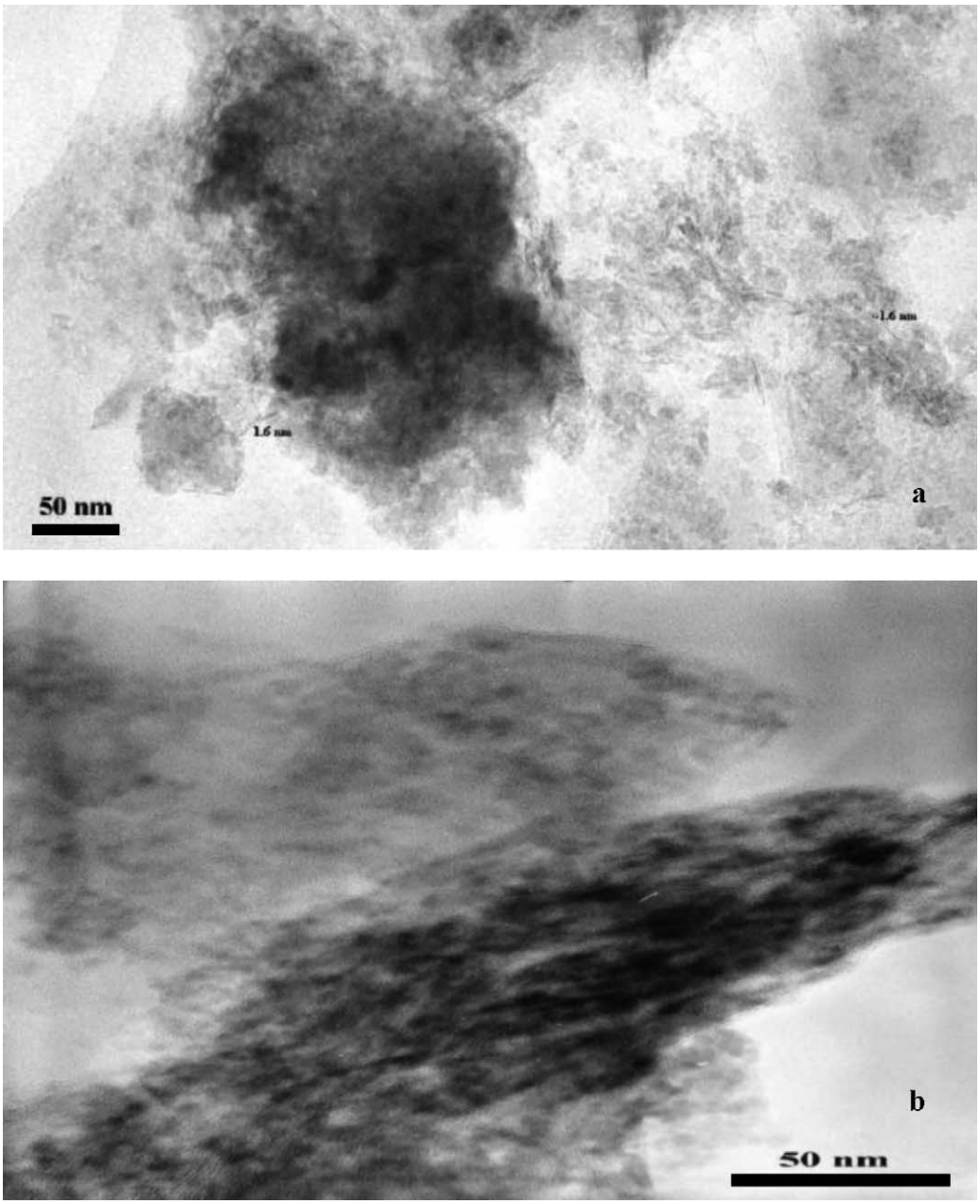

Fig. 7. High-resolution transmission electron imaging of the iron-pillared lalithe showing (a, b and c) the delaminated structure of the clay and (d) a goethite particle with its indexed electron diffraction pattern.

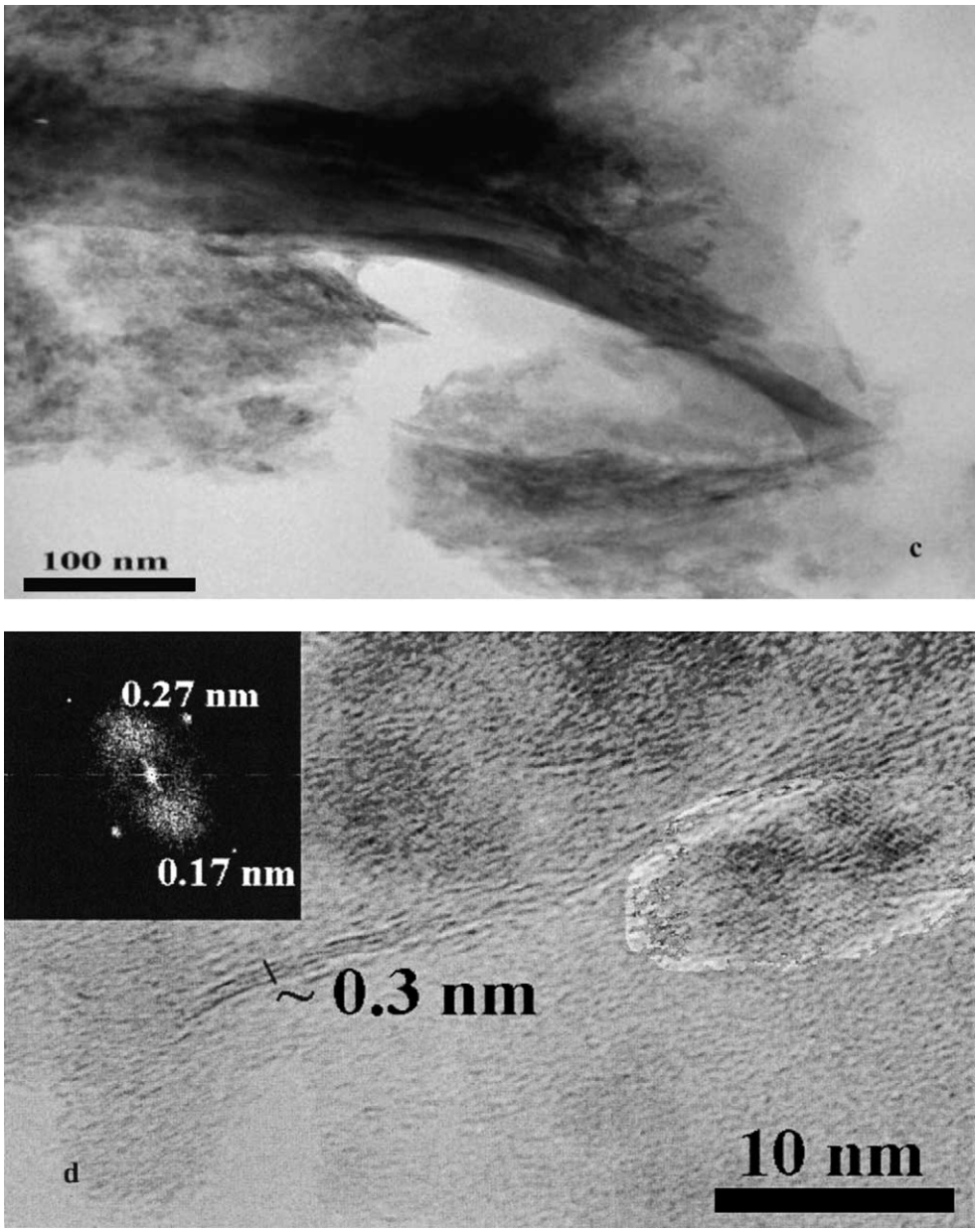

Fig. 7. (*Continued*).

3.3. Thermal stability of the intercalated clay

The isotherms obtained by adsorption of N_2 at 77 K and the porous distributions of the clays calcined at different temperatures are respectively presented in Figs. 4 and 5. The isotherms between 295 and 773 K are of type II according to the BET classification. Hysteresis was connected to the presence of macropores and the capillary condensation in the later ones. These isotherms were characteristic of a bimodal distribution with a well-developed microporosity and a sharp

Table 5
Textural characteristics of the intercalated clay calcined at different temperatures

Calcination temperature (K)	Specific surface area (BET) ($m^2\,g^{-1}$)	Micropores		Average diameter of the pores (Å)
		Surface area ($m^2\,g^{-1}$)	Volume ($cm^3\,g^{-1}$)	
Uncalcined	260	85.7	40	25.2
573	269	35.6	20	26.7
623	230	24.0	10	27.5
773	180	4.5	1	33.0

distribution of macropores. The size of the micropores was approximately 18 Å and that of the macropores 40 Å. These values were typical of pillared clay materials delaminated with the so-called *house-of cards* structure. With temperature, the microporosity decreased continuously whereas the macropore structure was not affected. This clearly appeared in Table 5 where the calculated micropores surface areas and volumes are given. Cylindrical pores have been considered for these calculations. The specific surface area between 573 and 623 K increased slightly instead of decreasing. This should be due to the concomitant departure of the water molecules present with the pillars in the interlayer space. The X-ray diffraction powder patterns of the heat-treated samples have been recorded (Fig. 6). We can see that the relative intensity of the $d_{(0\,0\,1)}$ decreased with temperature whereas it was slightly reduced. The *d*-spacing around 11 Å (near 9° (2θ)) appeared in the spectra of the heated samples. It has been attributed to a partially collapsed phase [7,23]. The peaks characteristic of the layers ($d = 4.47$, 4.05, 3.33, 3.21 and 2.52 Å) did not strongly evaluate with temperature which confirmed that the collapse of the pillared clay may be attributed to the sintering of the pillars, the silicate structure remaining almost the same.

3.4. Transmission electron microscopic study of the intercalated clay

The pillared sample has been studied by transmission electron microscopy. Four micrographs representative of the material are presented in Fig. 7. They showed the presence of stackings of clay layers distributed in a disorganized way. Such arrangements are typical of delaminated clays that confirmed the porosity data obtained. Interfoliaceous spacings measured were not uniform and vary from 3 to 16 Å, showing that the distribution of the iron cationic polymer species within the particles was inhomogeneous (Fig. 7a–d). Some layers were fully expanded while others remained unaffected. Although most of the solid was under this form with a relatively uniform composition, some very small particles (around 10 nm) containing only iron oxide have been detected (Fig. 7d). The indexed electron diffraction pattern corresponding to these particles showed that they consisted of goethite FeO(OH). The presence of this phase, which formed from ferrihydrite [24], was expectable and should be formed in the course of intercalation process when delamination occurred. However, the Mössbauer data, which identified only one doublet with a relatively narrow line with, tend to show that it was rather minor.

4. Conclusion

The Algerian natural bentonite appeared to be a suitable starting material for the preparation of iron-pillared clay catalysts. An optimized intercalation process applied to this purified material called lalithe enabled to obtain a delaminated iron-clay with a high specific surface area of 260 $m^2\,g^{-1}$ and an interplanar spacing of about 16 Å. The solids appeared highly delaminated with a macroporosity characterized by 40 Å pores.

The thermal stability study has shown that the obtained material was rather comparable to other iron-pillared clays. The macrostructure appeared rather stable and a relatively high surface area was maintained up to 773 K. However, the microporosity strongly decreased before the latter temperature. This instability should be related to the rather inhomogeneous distribution of the pillars within the clay as shown by transmission electron microscopy.

The study showed that it was possible to prepare from lalithe new materials with characteristics that make them suitable for catalytic applications. Such applications, which are under study, should allow the valorization of the former inexpensive material.

References

[1] D.E.W. Vaughan, Catal. Today 2 (1988) 187.
[2] M. Kojima, R. Hartford, C.T. O'Connor, J. Catal. 128 (1991) 487.
[3] S.M. Bradley, R.A. Kydd, J. Catal. 141 (1993) 239.
[4] F. Mokhtari, Thèse de Magister, University of Oran, Algérie, 1993.
[5] J.P. Chen, M.C. Hausladen, R.T. Yang, J. Catal. 151 (1995) 135.
[6] D.W. Thompson, N.M. Tahir, Colloids Surf. 60 (1991) 369.
[7] E.G. Rightor, M.S. Tzou, T.J. Pinnavaia, J. Catal. 130 (1991) 29.
[8] R.T. Yang, J.P. Chen, E.S. Kikkinides, L.S. Chengand, E. Cichanowiczt, Ind. Eng. Chem. Res. 31 (1992) 1440.
[9] L.S. Belaroui, F. Belkhadem, A. Bengueddach, in: IV Colloque Franco-Maghrébin de Catalyse, Lille, France, 1996, p. 201.
[10] L.S. Belaroui, F. Belkhadem, A. Bengueddach, IV Congrès de la Société Algérienne de Chimie, Tlemcen, Algérie, 1997, p. CO2.
[11] A.B. Bourlinos, M.A. Karakassides, A. Simopoulos, D. Petridis, Chem. Mater. 12 (2000) 2640.
[12] L.S. Belaroui, F. Belkhadem, J.M.M. Millet, A. Bengueddach, GECAT, Ile d'Oleron, France, 2001, p. 6.
[13] F. Bergaya, P. Gallot, R. Setton, H. Van Damne, Clays controlling the environment, in: Proceedings of the 11th International Conference on Clays, Adelaide, Australia, 1995, p. 151.
[14] H. Bernier, L.F. Admai, P. Grange, Appl. Catal. 77 (1991) 269.
[15] A. Matrod, Ph.D. Thesis, University of Montpellier, France, 1985.
[16] G.J.J. Bartley, R. Burch, Appl. Catal. 19 (1985) 175.
[17] E.M. Farfan-Torres, E. Sham, P. Grange, Catal. Today 15 (1992) 515.
[18] B.M. Choudary, S. Shobhapani, N. Narender, Catal. Lett. 19 (1993) 299.
[19] P. Aldridge, J.R. McLaughlin, C.G. Pope, J. Catal. 30 (1973) 409.
[20] L. Forni, Catal. Rev. 8 (1973) 65.
[21] J. Sanchez-Valente, J.M.M. Millet, L. Fournes, F. Figueras, Hyperfine Interact. 131 (2000) 43.
[22] S. Yamanaka, M. Hattori, in: R. Burch (Ed.), Catalysis Today, vol. 2, Elsevier, Amsterdam, 1988.
[23] L.V. Govea, H. Steinfink, Chem. Mater. 9 (1997) 849.
[24] A. Hamzaoui, A. Mgaidi, A. Megriche, M. El Maaoui, Ind. Eng. Chem. Res. 41 (21) (2002) 5226.